Mon. Not. R. Astron. Soc. **000**, 1–?? (2002) Printed 28 October 2014 (MN LATEX style file v2.2)

# Astro & cosmo-chemical consequences of accretion bursts I: the D/H ratio of water

James E. Owen⋆ and Emmanuel Jacquet†
*Canadian Institute for Theoretical Astrophysics, 60 St. George Street, Toronto, M5S 3H8, Canada.*

arXiv:1410.6844v1 [astro-ph.SR] 24 Oct 2014

28 October 2014

**ABSTRACT**

The D/H ratio of water in protostellar systems is a result of both inheritance from the parent molecular cloud and isotopic exchange in the disc. A possibly widespread feature of disc evolution, ignored in previous studies, is accretion bursts (or FU Orionis outbursts), which may thermally process a large fraction of the water. One proposed underlying mechanism for FU Orionis outbursts relies on the presence of a magnetically dead zone. Here we examine the evolution of $(\mathrm{D/H})_{\mathrm{water}}$ in 1D simulations of a disc's evolution that include dead zones and infall from an envelope with given D/H ratio in the infalling water ($\sim 10^{-3}$), and compare the results with similar calculations without dead zones. We find that the accretion bursts result in a significantly lower $(\mathrm{D/H})_{\mathrm{water}}$ ratio and a more extended region (radius up to $\sim 1-3$ AU) where water is equilibrated with hydrogen gas ($\mathrm{D/H}=2\times10^{-5}$), when compared to burst-free models. Solar system constraints suggest that our solar nebula either experienced no accretion bursts and had a Schmidt number $\lesssim 0.2$ or had a Schmidt number closer to "nominal" values ($\sim 1$) and experienced several accretion bursts. Finally, future observations of $(\mathrm{D/H})_{\mathrm{water}}$ in protoplanetary discs will allow inferences about angular momentum properties of the disc during disc building and the role of accretion bursts.

**Key words:** accretion, accretion discs - magnetohydrodynamics (MHD) - stars: pre-main sequence - planetary systems: protoplanetary discs - astrochemistry - comets: general

## 1 INTRODUCTION

While most observed protoplanetary discs display accretion rates of order $10^{-8\pm1}$ $\mathrm{M_\odot\ yr^{-1}}$ (Hartmann et al. 1998; Ercolano et al. 2014), some objects, in particular FU Orionis systems (e.g. Hartmann & Kenyon 1996), have exhibited episodes of enhanced accretion up to $\sim 10^{-4}$ $\mathrm{M_\odot\ yr^{-1}}$ (Audard et al. 2014) over observed time-scales of 10-100 years. It has been hypothesised that *all* protostellar systems actually undergo such episodic accretion, equating to a small fraction (the "duty cycle") of their total lifetime, possibly concentrated in their early stages (Kenyon et al. 1990). Indeed this would alleviate the apparent discrepancy between the low observed accretion rates and that required to achieve the final mass of the protostars (Kenyon et al. 1990; Evans et al. 2009; Audard et al. 2014).

Although the mechanism underlying FU Orionis outbursts has not been established to date (Audard et al. 2014), a presently popular class of model uses as its only ingredients the two currently favoured drivers of transport in protoplanetary disks, namely the magnetorotational instability (MRI; Balbus & Hawley 1998) and the gravitational instability (Lodato & Rice 2004, 2005; Durisen et al. 2007). The "gravo-magnetic cycle", as it has come to be called (Martin & Lubow 2011, 2013, 2014), relies on the fact that a disc with a "normal" density is typically too cold ($\sim 100-300$ K) and too dense for its mid-plane to be sufficiently ionised to trigger the MRI, giving rise to a *dead zone*. As the disc is gravitationally stable at such densities, accretion will only be possible in the surface layers where X-ray/UV (or cosmic ray) ionisation keeps the MRI alive (Gammie 1996). However, a steady-state situation cannot be achieved and mass accumulates in the dead zone, until gravitational instability sets in, raising the disc's mid-plane temperature ($T_m$). Near $T_m \sim 800-1200$ K, thermal ionisation triggers the MRI throughout the entire thickness of the disc, resulting in an accretion burst which lasts $\sim 10^3-10^4$ years (e.g. Armitage, Livio, & Pringle 2001; Zhu et al. 2010; Ohtani et al. 2014; Owen & Armitage 2014). Once the previously accumulated mass is dumped on the proto-star, the disc returns to the initial "low state" (or quiescent state). The cycle may then resume, with a duty cycle $\lesssim 1$ % at low in-

⋆ E-mail: jowen@cita.utoronto.ca
† E-mail: ejacquet@cita.utoronto.ca

© 2002 RAS

fall rates ($\sim 10^{-8}$ $M_\odot$ $yr^{-1}$ ) up to $\sim 30$ % at high infall rates ($\sim 10^{-6}$ $M_\odot$ $yr^{-1}$ ).

The significant changes in the disc's temperature and luminosity during such an accretion burst can chemically process a large fraction of the disc material. Several previous studies have shown the impact of accretion bursts on the chemical evolution of the envelope and disc. Lee (2007); Vorobyov et al. (2013) studied the impact of accretion busts on the CO chemistry in the envelopes, in particular the large increase in luminosity, and found that repeated bursts could lead to repeated freeze-out cycles. These evolutionary CO cycles lead to possible observational evidence of accretion outbursts in young star forming cores (Kim et al. 2011, 2012). Additionally, Visser & Bergin (2012) used 'single-point' models to study the impact of accretion bursts on the local evolution of various chemical species in the envelope, indicating that the outcome depends delicately on the balance between burst and chemical time-scales. However, what has not been considered in great detail is that this processed material can then be transported to smaller radii in the disc by advection and to larger ones by turbulent diffusion. These effects, which may persist for significantly longer than the duration of the bursts, may lend themselves to observable diagnostics; whether for extrasolar systems, e.g. with the increased resolution and sensitivity offered by *ALMA* and *Herschel*, or our own solar system, taking advantage of the rich body of cosmochemical evidence. To this end, in this series we set out to investigate the chemical consequences of accretion bursts.

An astrochemically abundant species of choice in this regard is water (Hogerheijde et al. 2011), and in particular its D/H ratio (van Dishoeck et al. 2014; Ceccarelli et al. 2014). Observations of the interstellar medium and pre-stellar cores suggest that water starts deuterium-rich ($D/H \gtrsim 10^{-3}$; Robert et al. 2006; Ceccarelli et al. 2014). Yet bulk chondrites and comets (with a further *in situ* measurement to come for comet Churyumov-Gerasimenko Hässig et al. 2013) in our solar system display lower $(D/H)_{water}$ ratios (around $1 - 3 \times 10^{-4}$), although some micron-scale D-rich hotspots in clays of the Semarkona chondrite do reach $(D/H)_{water} \gtrsim 2 \times 10^{-3}$ (Deloule, Robert, & Doukhan 1998; Piani 2012; Piani, Robert, & Rémusat 2014). This in turn is much higher than the protosolar value (essentially that of molecular hydrogen) of $2 \times 10^{-5}$ (Geiss & Gloeckler 2003), and reaction kinetics prohibit the conversion of low $(D/H)_{water}$ ratios to higher values in the protoplanetary disc (Drouart et al. 1999). The current interpretation is that the solar system inherited its water from the parent molecular cloud (Visser et al. 2009; Visser, Doty, & van Dishoeck 2011), and that this water *partially* exchanged its deuterium with the nebular gas (Yang, Ciesla, & Alexander 2013). Coupling this deuterium exchange with mixing throughout the disc produced the range of intermediate $(D/H)_{water}$ values we now observe (Drouart et al. 1999; Mousis et al. 2000; Hersant, Gautier, & Huré 2001; Jacquet & Robert 2013; Yang, Ciesla, & Alexander 2013; Albertsson, Semenov, & Henning 2014). The bottom line is that the (D/H) ratio of water is a sensitive tracer of infall, temperature and turbulent mixing conditions.

All previous studies of the $(D/H)_{water}$ ratio assumed a constant turbulence level (often parametrised in terms of the Shakura & Sunyaev $\alpha$, Shakura & Sunyaev 1973), and thus could not reproduce the gravo-magnetic cycle, and had no accretion outbursts. Additionally, only Yang, Ciesla, & Alexander (2013) considered the effects of infall, during which most of the outbursts are expected to take place (Armitage, Livio, & Pringle 2001; Zhu, Hartmann, & Gammie 2010), along with the subsequent disc evolution. Jacquet & Robert (2013) presented steady-state analytical calculations, indicating that in such types of model, a high efficiency of turbulent diffusion - with a Schmidt number $Sc$ of 0.2 or smaller - until the snow line and beyond would be required to account for the smallness of the $(D/H)_{water}$ ratio of carbonaceous chondrites and the Earth relative to Oort cloud comets; but as yet the realism of such a small Schmidt number is unclear (Jacquet & Robert 2013). However, as isotopic exchange is most efficient for temperatures above $\sim 400 - 800$ K (the "equilibration temperature"[1], Yang, Ciesla, & Alexander 2013; Jacquet & Robert 2013), clearly, outbursts, which may reach temperatures in excess of 1000 K, could significantly impact the $(D/H)_{water}$ profile of protoplanetary disc and possibly account for the low $(D/H)_{water}$ ratios of carbonaceous chondrites.

In this work, we examine the effect of accretion outbursts arising from the gravo-magnetic limit cycle on the evolution of the (D/H) ratio of water using numerical models presented in Section 2. Since this process has not been studied before, to gain insight we perform numerical experiments where the disc experiences a steady infall rate for the entire simulation (Section 3). Secondly, we perform more realistic evolutionary calculations which include a disc building phase for a few hundred-thousand years followed by a stage of isolated evolution for several million years, that are meant to represent the evolution of an actual protoplanetary disc, e.g. the solar nebula (Section 4). The implications are then discussed in Section 5 and the conclusions summarized in Section 6.

## 2 ONE-DIMENSIONAL DISC MODEL

In order to investigate the effect of accretion bursts on the chemical evolution of the $(D/H)_{water}$ ratio we adopt a simple one-layer approach (Owen & Armitage 2014). Our model is a modified version of that originally presented by Armitage, Livio, & Pringle (2001) to study the impact of dead-zones in protoplanetary discs and associated accretion bursts, where we additionally include radial transport of heat by radiation and turbulence (see Owen & Armitage 2014). Here we extend the model to include the transport of water due to advection and turbulent diffusion as well as the chemical evolution of the $(D/H)_{water}$ ratio.

### 2.1 Gas component

The evolution of the surface density $\Sigma^g$ for a disc around a forming star, with a dead-zone is given by (e.g. Armitage,

[1] Its value depends somewhat on disc parameters, in particular $\alpha$, or the opacity, hence the range quoted.

Livio, & Pringle 2001):

$$\frac{\partial \Sigma^g}{\partial t} = \frac{3}{R}\frac{\partial}{\partial R}\left\{R^{1/2}\frac{\partial}{\partial R}\left[\left(\nu_{\rm MRI}\Sigma^g_{\rm ac} + \nu_{\rm SG}\Sigma^g\right)R^{1/2}\right]\right\} + \dot{\Sigma}^g_{\rm in} \tag{1}$$

where $\nu_i$ is the kinematic viscosity due to the MRI or self-gravity which we detail in Section 2.1.1 and $\dot{\Sigma}^g_{\rm in}$ is the rate of material falling onto the disc. $\Sigma^g_{\rm ac}$ is the surface density that is 'MRI active' and is given by:

$$\Sigma^g_{\rm ac} = \begin{cases} \Sigma^g & \text{if } T_m > T_{\rm crit} \text{ or } \Sigma^g < 2\Sigma_{\rm layer} \\ 2\Sigma_{\rm layer} & \text{otherwise} \end{cases} \tag{2}$$

For all our models where we include a dead-zone (and hence accretion bursts) we choose $T_{\rm crit} = 800\,{\rm K}$ and $\Sigma_{\rm layer} = 10^2\,{\rm g\,cm^{-2}}$. In simulations where we do not include a dead-zone (and thus no accretion bursts) we set $\Sigma^g_{\rm ac} = \Sigma^g$.

The evolution of the temperature at the mid-plane of the disc is given by (Owen & Armitage 2014):

$$\begin{aligned}\frac{\partial T_m}{\partial t} &= -v_R\frac{\partial T_m}{\partial R} + \frac{1}{\Sigma^g}\left[\frac{\Gamma}{C_p} - \frac{T_m}{\gamma\Theta R}\frac{\partial}{\partial R}\left(RF_\Theta\right)\right] \\ &\quad - \left(\frac{2H}{\Sigma^g R C_p}\right)\frac{\partial}{\partial R}\left(RF_R\right)\end{aligned} \tag{3}$$

where $C_p$ is the heat capacity at constant pressure, $\gamma$ is the ratio of specific heats and $H = c_s/\Omega$ is the scale height of the disc, with $\Omega$ the Keplerian angular velocity and $c_s$ the isothermal sound speed. $\Theta$ is the 'potential temperature' of the disc's mid-plane and following Owen & Armitage (2014) we define it as:

$$\Theta \propto T_m\left(\Sigma^g\Omega\right)^{\frac{2(1-\gamma)}{1+\gamma}}, \tag{4}$$

noting that Equation 3 is independent of the choice of scaling for the potential temperature.The net heating rate ($\Gamma$) is given by:

$$\Gamma = \frac{9}{4}\nu\Sigma^g_{\rm ac}\Omega^2 - \frac{16}{3\tau}\sigma_b T_m^4, \tag{5}$$

where $\sigma_b$ is the Stefan-Boltzmann constant and $\tau = \Sigma^g\kappa/2$ is the vertical optical depth, with $\kappa$ the opacity. The two fluxes $F_\Theta$ & $F_R$ are the radial heat fluxes due to turbulence and radiation respectively; which are given by:

$$F_\Theta = -\frac{3\nu\Sigma^g}{Pr}\frac{\partial\Theta}{\partial R}, \tag{6}$$

where $Pr$ is the Prandtl number (in most calculations we take $Pr = 10$, the preferred value suggested by Owen & Armitage 2014), and

$$F_R = -\frac{4acT_m^3}{\kappa\rho}\frac{\partial T_m}{\partial R}, \tag{7}$$

with $a$ the radiation constant, $c$ the speed of light and $\rho$ the mid-plane density. For our model we adopt the Bell et al. (1997) opacities and Equation 3 is integrated as described in Owen & Armitage (2014).

Our heating term (Equation 5) does not account for stellar irradiation, which is known to dominate the heating in the outer disc (e.g. Kenyon & Hartmann 1987; Chiang & Goldreich 1997; D'Alessio, Calvet, & Hartmann 2001). Therefore, we do not allow the disc's temperature to drop below what would be obtained for a passively heated disc given by:

$$T_p = T_{\rm 1AU}\left(\frac{R}{1\ {\rm AU}}\right)^{-1/2} \tag{8}$$

We set $T_{\rm 1AU}$ to:

$$T_{\rm 1AU} = 200\,{\rm K}\left[\frac{8}{9}\left(\frac{M_*}{1\,{\rm M}_\odot}\right) + \frac{1}{9}\right]^{1/4} \tag{9}$$

where the mass scaling is identical to that adopted by Zhu et al. (2010), based on a fit to a T Tauri star's birth-line from Kenyon & Hartmann (1995). Finally, the temperature is also restricted to be no less than 10 K at very large radius, to account for heating from the surrounding star-forming region. In all calculations we assume an ideal equation of state with $\gamma = 7/5$ and a mean molecular weight ($\mu$) of 2.35 amu as the majority of the disc material we are interested in remains molecular and neutral.

### *2.1.1 Viscosity and Self-Gravity*

We treat the viscosity using an 'alpha' model such that:

$$\nu_i = \alpha_i c_s H. \tag{10}$$

For MRI turbulence we set $\alpha_{MRI} = 0.01$ and for angular momentum transport due to self-gravity we set $\alpha_{\rm SG}$ to

$$\alpha_{\rm SG} = \begin{cases} 0.01\left(\frac{Q^2_{\rm crit}}{Q^2} - 1\right) & \text{if } Q \leqslant Q_{\rm crit} \\ 0 & \text{if } Q > Q_{\rm crit} \end{cases} \tag{11}$$

where $Q$ is the Toomre parameter (Toomre 1964) given by:

$$Q = \frac{c_s\Omega}{\pi G\Sigma^g} \tag{12}$$

The form of $\alpha_{SG}$ is not important and is merely designed to keep $Q \sim Q_{\rm crit} = 2$ (e.g. Lin & Pringle 1987, 1990; Zhu et al. 2010) as suggested by simulations of self-gravitating discs (e.g. Lodato & Rice 2004, 2005).

## 2.2 Water component

We treat the water component of the disc as a passive scalar species, such that it is advected along with the gas and can diffuse with respect to the gas due to turbulence. Thus, the evolution of the water component is given by (e.g. Jacquet & Robert 2013; Yang, Ciesla, & Alexander 2013):

$$\begin{aligned}\frac{\partial \Sigma_i}{\partial t} = \frac{1}{R}\frac{\partial}{\partial R}\Bigg[&\frac{R}{Sc}\left(\nu_{\rm MRI}\Sigma^g_{\rm ac} + \nu_{SG}\Sigma^g\right)\frac{\partial}{\partial R}\left(\frac{\Sigma_i}{\Sigma^g}\right) \\ &- R\Sigma_i v_R\Bigg] + \dot{\Sigma}_i\end{aligned} \tag{13}$$

where we evolve Equation 13 for the two water species $H_2O$ and HDO. $\dot{\Sigma}_i$ represents both infall onto the disc and the chemical evolution of the two species. Since the purpose of this work is to understand whether accretion bursts affect the evolution of the $({\rm D/H})_{\rm water}$ ratio rather than make detailed predictions, we do not attempt to model a full chemical network but adopt the simple model proposed by Jacquet & Robert (2013) based on Lécluse & Robert (1994), where the $({\rm D/H})_{\rm water}$ ratio in water evolves as:

$$\frac{\rm d}{{\rm d}t}\left(\frac{D}{H}\right) = k_-(T)n_g\left[\left(\frac{D}{H}\right)_{\rm eq}(T) - \left(\frac{D}{H}\right)\right] \tag{14}$$

where $n_g$ is the gas number density at the disc's mid-plane, $k_-(T)$ is the rate constant for the deuteration of water given

by (Lécluse & Robert 1994)

$$k_-(T) = 2 \times 10^{-22}\ \mathrm{cm^3\ s^{-1}}\ \exp\left[-\left(\frac{5170\ \mathrm{K}}{T}\right)\right] \quad (15)$$

and $(\mathrm{D/H})_{\mathrm{eq}}$ is the equilibrium D/H ratio at a given temperature, which we take from Richet, Bottinga, & Janoy (1977) assuming the D/H ratio in the background molecular hydrogen dominated disc is $2 \times 10^{-5}$. The latter values were found by Yang, Ciesla, & Alexander (2013) to agree reasonably well with the values obtained from their more detailed chemical network. In all calculations we assume, like Yang, Ciesla, & Alexander (2013), that the $(\mathrm{D/H})_{\mathrm{water}}$ ratio of the in-falling primordial water is $10^{-3}$.

### 2.3 Infall Models

The infall profile adopted depends on the evolutionary model (steady infall vs. disc building calculations). For the steady infall problem we use a Gaussian infall profile which peaks at a radius $R_{\mathrm{in}}$ and has standard deviation $0.1R_{\mathrm{in}}$ (e.g. Owen & Armitage 2014). For the full evolutionary calculations, where we account for disc building from a uniformly rotating collapsing core, we follow Dullemond, Natta, & Testi (2006); Yang & Ciesla (2012); Yang, Ciesla, & Alexander (2013) and adopt the Hueso & Guillot (2005) infall profile:

$$\dot{\Sigma}^g = \frac{\dot{M}}{8\pi R_c(t)^2}\left(\frac{R}{R_c(t)}\right)\left[1-\left(\frac{R}{R_c(t)}\right)^{1/2}\right], \quad (16)$$

where the instantaneous centrifugal radius ($R_c$) of the infalling material is given by angular momentum balance:

$$R_c(t) = 1.3\,\mathrm{AU}\left(\frac{\Omega_c}{10^{-14}\,\mathrm{s^{-1}}}\right)^2\left(\frac{T_c}{15\,\mathrm{K}}\right)^{-4}\left(\frac{M(t)}{0.5\,\mathrm{M_\odot}}\right)^3 \quad (17)$$

where $\Omega_c$ is the core's rotation rate (considered to be constant in space and time), $T_c$ is the temperature of the core and $M(t)$ is the mass of the star & disc. Finally, we assume the core follows an isothermal inside-out collapse (e.g. Shu 1977) and use a constant infall rate of

$$\dot{M} = 0.975\frac{c_c^3}{G} \quad (18)$$

until the core mass is fully depleted, where $c_c$ is the sound speed for gas at a temperature of $T_c = 15$K in all calculations (as in Yang, Ciesla, & Alexander 2013).

### 2.4 Numerical Method

Our numerical code is based on the method detailed in Owen (2014a); Owen & Armitage (2014) where advective fluxes are reconstructed using a second order method and a Van-Leer limiter. Equations 3 & 1 are integrated explicitly using a scheme that is second order in space and first order in time using a staggered mesh and finite volume operators. In order to evolve the transport and chemistry of the water content we make use of operator splitting: First, equation 13 without the chemical evolution terms is integrated explicitly using a scheme that is second order in space and first order in time. Secondly the chemical evolution is evolved by integrating Equation 14 using an implicit update, such that:

$$\frac{(D/H)^{n+1}-(D/H)^n}{\Delta t} = (k_- n_g)^{n+1/2}\left[\left(\frac{D}{H}\right)^{n+1}_{\mathrm{eq}} - \left(\frac{D}{H}\right)^{n+1}\right] \quad (19)$$

such a scheme is stable for equation that are both stiff and non-stiff over a simulation domain and thus appropriate for our problem. The simulations are initialised with the gas surface density set to the numerical floor of $\Sigma^g = 10^{-20}\mathrm{g\ cm^{-2}}$ and the temperature set to 10 K. We use a non-uniform radial grid, using power-law spacing (Owen 2014a). At the inner boundary we use a zero-torque boundary condition for the gas surface density and a free outflow boundary for the water species. For our steady infall calculations we use 200 cells spaced between 0.1 and 66.8 AU and at the outer boundary we use a zero-flux boundary condition for both the gas and water species. Whereas for the disc building calculations we use 400 cells spaced between 0.047 AU and 6685 AU, at the outer boundary we use a zero shear boundary condition for the gas and a free-outflow boundary condition for the water.

In Appendix A, we benchmark our simplified scheme against the results of the more complicated chemical network used by Yang, Ciesla, & Alexander (2013) and find very good agreement. Therefore, our simple scheme is appropriate for analysing the impact of accretion bursts on the D/H ratio in water.

## 3 STEADY INFALL CALCULATIONS

In order to better understand the effects of accretion bursts we consider a setup with steady infall; where the star's mass does not grow with time and is fixed to $M_* = 1\ \mathrm{M_\odot}$ . Such calculations have been previously used to study the properties of the accretion bursts themselves (Armitage, Livio, & Pringle 2001; Zhu et al. 2009; Owen & Armitage 2014) as they reach a steadily repeating limit cycle. Initially, only gas falls onto the disc and it reaches a steady-limit cycle after approximately 0.3-0.6 Myr. After 1 Myr we then allow both water and gas to fall onto the disc and evolve the calculation for a further 3 Myr. We perform large sets of calculations, where in all sets we vary the infall rate from $6.3 \times 10^{-9}$ to $10^{-5}\ \mathrm{M_\odot\ yr^{-1}}$ and the infall radius from 0.32 to 32 AU. We run one set of calculations with no dead-zone and thus no accretion bursts. Additionally, we run five further sets which include accretion bursts: three have a Prandtl number of 10 (the theoretically preferred value of Owen & Armitage 2014) and vary the Schmidt number taking $Sc = 0.3$, 1.0 & 3.0; finally we run two sets with a Schmidt number of 1.0 but Prandtl numbers of 1 & 100.

### 3.1 Results

In Figure 1, we show the radial distribution of the D/H ratio in water 0.5 Myr after the water has been introduced into the disc (we plot the profile during quiescence as the D/H ratio shows a transient during the burst) for a simulation with $\dot{M} = 1.2 \times 10^{-6}\ \mathrm{M_\odot\ yr^{-1}}$ and $R_{\mathrm{in}} = 11.3$ AU in the six sets of calculations.

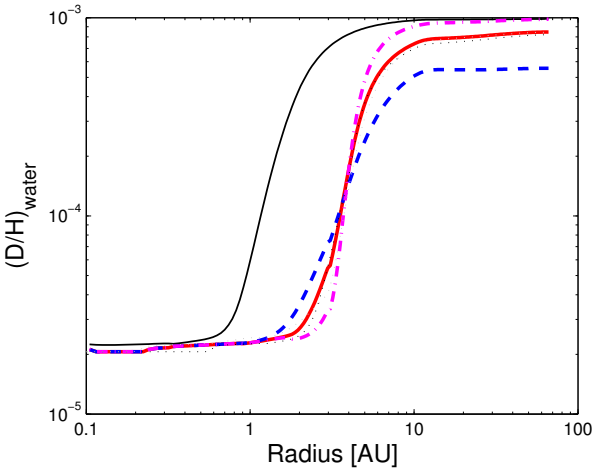


**Figure 1.** The $(D/H)_{water}$ profile after 0.5 Myr of evolution in a disc with a steady infall rate of $\dot{M} = 1.2 \times 10^{-6}$ $M_\odot$ $yr^{-1}$ occurring at $R_{in} = 11.3$ AU. The thin solid line shows the result with no dead zone (and therefore no accretion bursts). The thick lines show simulations with accretion bursts with Schmidt numbers of (0.3 - dashed, 1.0 - solid & 3.0 - dot-dashed). The thin dotted lines represent calculations with accretion bursts and a Schmidt number of 1.0 but Prandtl numbers of 1.0 (black) & 100.0 (grey).

These profiles clearly show that accretion bursts have a strong impact on the D/H ratio distribution. With accretion bursts the radius at which the D/H ratio reaches the fully equilibrated value of $\sim 2 \times 10^{-5}$ (the "equilibration radius"; where the equilibration time-scale is comparable to the transport time-scale c.f. Jacquet & Robert 2013) increases from roughly 1 AU to 3 AU. Additionally, it decreases the D/H ratio at large radius in the disc from the unprocessed value ($10^{-3}$) with no accretion bursts to $\sim 5 \times 10^{-4}$ with accretion bursts and a Schmidt number of 0.3. Finally, we note that the value of the Prandtl number makes little difference. This is likely due to the fact that while the Prandtl number does affect the individual properties of an accretion burst (e.g. duration) it does not effect the duty-cycle of the burst significantly (Owen & Armitage 2014) and hence the fraction of disc material processed by the accretion burst when averaged over a time-scale longer than the burst time-scale.

In Figures 2 & 3 we show the space-time evolution of the temperature (right-panel) and $(D/H)_{water}$ (middle-panel), along with the accretion rate evolution (left-panel). Figure 2 shows that the $(D/H)_{water}$ ratio quickly reaches a steady state distribution where the equilibration radius occurs at 1 AU (the temperature here is essentially due to viscous dissipation), in agreement with the analytic models of Jacquet & Robert (2013). However, Figure 3 shows that, in the presence of accretion bursts, the $(D/H)_{water}$ ratio never reaches a steady state; but like the accretion rate reaches a steadily repeating pattern, where incoming material is accreted into the dead zone region with a $(D/H)_{water} \approx 10^{-3}$, which is then equilibrated in the dead zone region when the disc goes through an accretion burst, which raises the temperature well above the equilibration temperature to $\sim 1000$ K. Thus, the dead zone is able to thermally process a larger fraction of the disc material, such that the equilibration radius is considerably further out than predicted by models that do not include accretion bursts. Furthermore, as well as being carried by advection along with the gas, this newly equilibrated water in the dead zone region can diffuse out to large radius ($\gtrsim 10$ AU) in the disc lowering the (time-independent) $(D/H)_{water}$ ratio. In the case with accretion bursts, this is more efficient than without because equilibration occurs at a larger radius.

### 3.2 Parameter study

In Figures 4 and 5 we show the $(D/H)_{water}$ ratio measured at different locations in the disc after 0.5 Myrs of evolution for the whole range of $\dot{M}$ and $R_{in}$ examined. Figure 4 shows the $(D/H)_{water}$ ratio at 1.0, 3.0, 10 & 30 AU for the simulation set with a Schmidt number of 1.0 and no accretion bursts. This shows that at high accretion rates and small infall radii, most of the in-falling water is equilibrated before it can be transported to large radii resulting in a fully equilibrated disc. At low accretion rates $\lesssim 3 \times 10^{-8}$ $M_\odot$ $yr^{-1}$ the disc is too cold to equilibrate the water except at very small radii ($\lesssim 1$ AU) and at intermediate values one gets a profile similar to that shown in Figure 1 where the water is equilibrated inside some radius, the equilibration radius, which is an increasing function of mass accretion rate. Essentially, the warmer the disc region onto which the infalling matter arrives, the more equilibrated the water of the disc as a whole will be.

The simulation set with accretion bursts and Schmidt number of 1.0 is shown in Figure 5 with the $(D/H)_{water}$ ratio measured at 1.0, 3.0, 10.0 & 30.0 AU after 0.5 Myr of evolution. This shows a similar trend with infall rate and infall radius as previously; however, with accretion bursts it is much more pronounced. Similarly, the general trend of larger equilibration radius and lower $(D/H)_{water}$ ratio at large radius in the specific case discussed above holds for the majority of the parameter space. Comparing these results with those found in Figure 4 indicates that for the majority of the parameter space of interest the terrestrial region will have equilibrated water. However, in order for the $(D/H)_{water}$ ratio to be reduced from primordial values at large radius requires infall rates $\gtrsim 3 \times 10^{-7}$ $M_\odot$ $yr^{-1}$ , which is expected to occur at early times (e.g. Hartmann et al. 1998). However, the reduced $(D/H)_{water}$ ratio at large radius does appear to sensitively depend on the infall radius, with $R_{in} \lesssim 3$ AU resulting in fully equilibrated water at large radius: essentially all the incoming water is thermally processed in the dead-zone before it is transported to large radius. Whereas with $R_{in} \gtrsim 3$ AU the $(D/H)_{water}$ ratio is only reduced from primordial values by a factor of $\sim 2$, where the equilibrated water at large radius comes from the turbulent diffusion of material processed in the dead-zone that has then be transported to larger radius.

## 4 DISC BUILDING AND EVOLUTION CALCULATIONS

We now consider calculations where we build the disc from a uniformly rotating core. Initially the star has a mass of 0.2 $M_\odot$ and the cloud core contains 0.8 $M_\odot$ . The cloud core then falls onto the disc as described in Section 2.3. Any

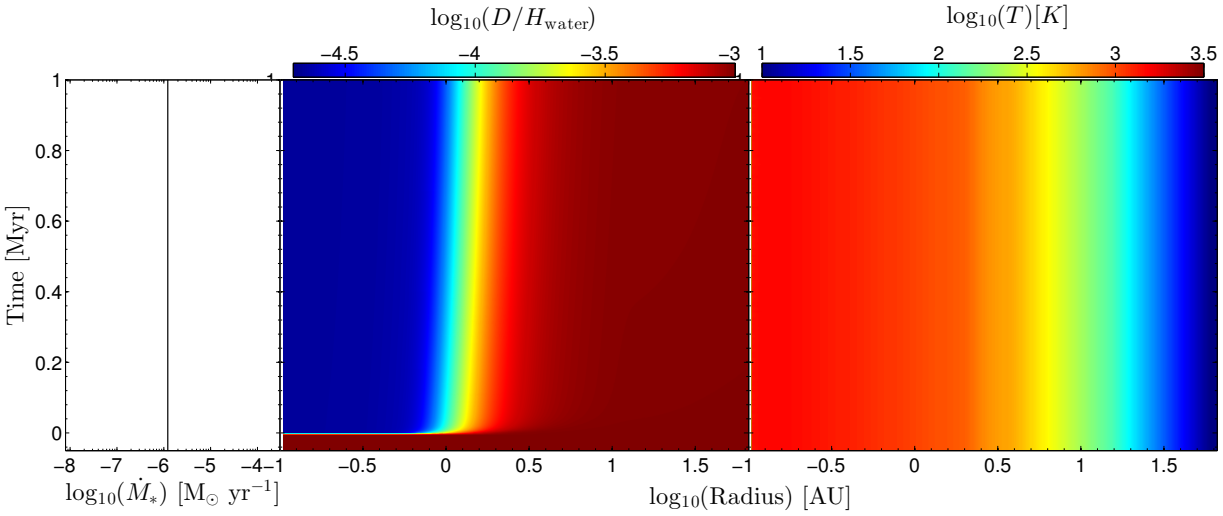


**Figure 2.** Evolution of a steady infall calculation with $\dot{M} = 1.2 \times 10^{-6}$ M$_\odot$ yr$^{-1}$ and $R_{\rm in} = 11.3$ AU with no dead zone and a Schmidt number of 1.0. The left-hand panel shows the accretion rate as a function of time. The middle panel is a space-time plot showing the evolution of the $(\rm D/H)_{water}$ ratio and the right panel is a space-time plot for the temperature evolution. Zero-time has been reset to the point at which water is introduced into the system.

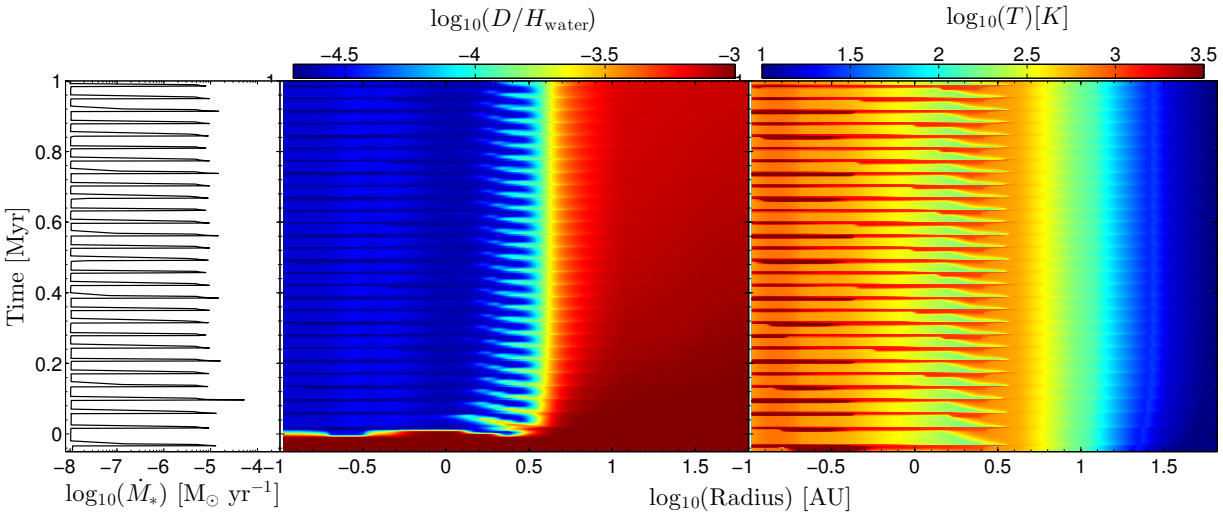


**Figure 3.** Same as Figure 2, for a steady infall calculation with $\dot{M} = 1.2 \times 10^{-6}$ M$_\odot$ yr$^{-1}$ and $R_{\rm in} = 11.3$ AU with accretion bursts and a Schmidt number of 1.0.

material that falls inside the inner boundary is automatically added to the star, whose mass is subject to an explicit update. Since we have seen above that the Prandtl number makes little difference to the results, we only perform calculations with $Pr = 10$. We then perform a series of simulations where we vary the cloud's rotation rate $\Omega_c$ between $8 \times 10^{-16}$ & $3.16 \times 10^{-13}$ s$^{-1}$, the Schmidt number between 0.1 & 10 and whether or not the disc experiences accretion bursts.

### 4.1 Results

In Figure 6, we show how the individual components (star, cloud core & disc) in our disc building calculations evolve during the simulation for a model with $\Omega_c = 8.88 \times 10^{-15}$ s$^{-1}$. The top panel shows a model with no accretion burst and the bottom panel shows a simulation with accretion bursts. In this case infall takes approximately 0.2 Myr.

In the case with no accretion bursts the star rapidly approaches 1 M$_\odot$ after infall ceases and the disc remains below 0.1 M$_\odot$ for the majority of the evolution and steadily declines in a power-law fashion. However, in the case with accretion bursts, the dead zone traps material in the disc. This results in a more massive disc around 0.1-0.2 M$_\odot$ for

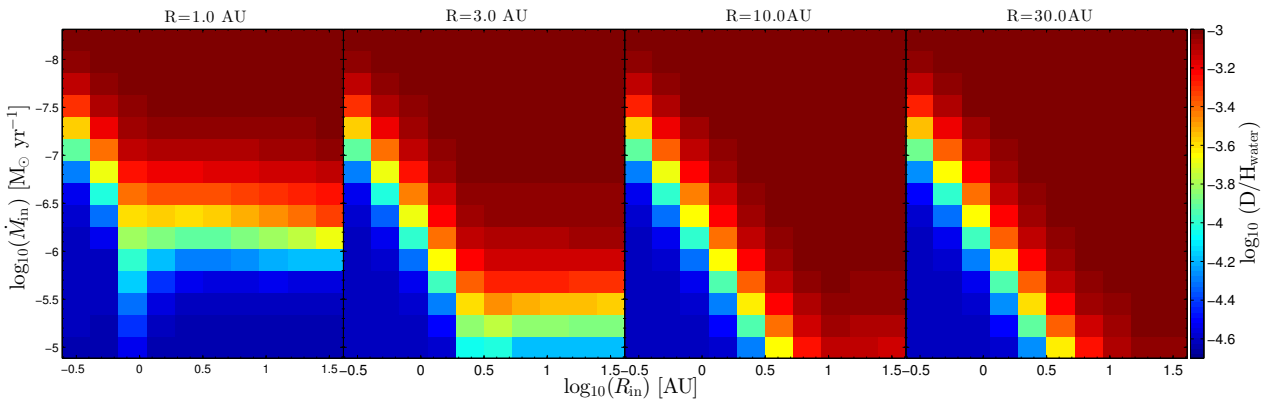


**Figure 4.** Colour maps showing the $(D/H)_{water}$ ratio at 1.0, 3.0, 10.0 & 30.0 AU in the protoplanetary disc with no dead-zone and a Schmidt number of 1.0 after of 0.5 Myrs of evolution.

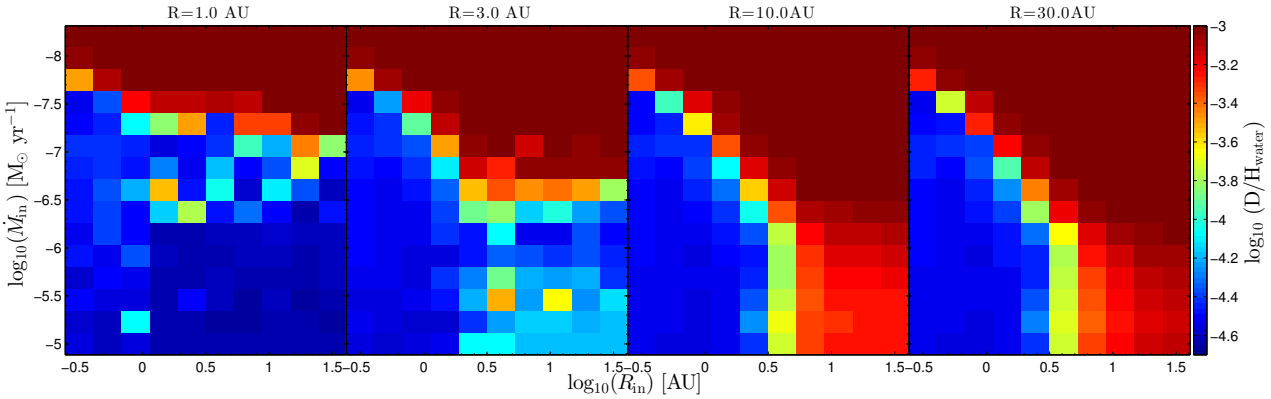


**Figure 5.** Colour maps showing the $(D/H)_{water}$ ratio at 1.0, 3.0, 10.0 & 30.0 AU in the protoplanetary disc with accretion bursts and a Schmidt number of 1.0 after 0.5 Myrs of evolution. The larger amplitude variations in the $(D/H)_{water}$ ratio in the predominately equilibrated regions is a measure of the temporal variability at a given location seen in Figure 3 and discussed above.

the majority of the evolution, which accretes material onto the star in rapid bursts. This evolution is similar to that found previously (e.g. Armitage, Livio, & Pringle 2001; Zhu, Hartmann, & Gammie 2010; Bae et al. 2013b) where discs that contain dead zones are generally more massive (and thus hotter) than discs that do not.

In Figures 7 & 8 we show the evolution of the accretion rate (left panel), centrifugal radius and snow-line radius taken at $T_M = 170$ K (thick dashed line and thick solid line respectively in middle and right panels), $(D/H)_{water}$ ratio (middle panel) and disc temperature (right panel) as a function of time of the calculations shown in Figure 6. Figure 7 shows the space-time evolution for a calculation with $\Omega_c = 8.88 \times 10^{-15}$ s$^{-1}$ and no accretion burst. The accretion rate evolution shows that once the infall onto the disc ceases the accretion rate drops dramatically; this coincides with a large decrease in disc temperature, which then slowly declines with time. The middle panel shows that the $(D/H)_{water}$ ratio has a plateau around 10 AU and declines at both large and small radius. This evolutionary track was seen by Yang, Ciesla, & Alexander (2013) and is also shown in our benchmark calculation discussed in the Appendix. At large radius this disc is primarily composed of material that fell at small radius into the hot disc and then was transported to large radius by decretion (e.g. Dullemond, Apai, & Walch 2006; Yang, Ciesla, & Alexander 2013). The water that fell at early times into the hot inner disc was equilibrated and then transported to large radius resulting in a $(D/H)_{water}$ ratio close to the equilibrated value at large radius (although this radius increases with time). At small radius the disc is hot enough to rapidly equilibrate the water, although the equilibration radius moves inwards with time as the disc temperature falls as the disc's mass decreases.

Figure 8 shows the same calculation, but this time with accretion bursts. In this case, once infall ceases the accretion rate reaches $\sim 10^{-8}$ M$_\odot$ yr$^{-1}$ , which then rapidly burst to $\sim 10^{-4}$ M$_\odot$ yr$^{-1}$ occasionally. While the evolution of the temperature and $(D/H)_{water}$ ratio is similar at very large radius to the calculation without accretion bursts with a region of equilibrated water that is transported to large radius by decretion. However, we see that the presence of a dead-zone and accretion bursts dramatically changes the $(D/H)_{water}$ ratio profile in the inner regions of the disc. We also see an individual accretion burst has a transient effect that lasts ∼0.5 Myr. Each accretion burst processes a large fraction of water in the disc, resulting in a lower peak $(D/H)_{water}$ ratio (as also seen in the steady infall calculations) and results in a equilibration radius that on average remains constant with time (at $\sim 1$ AU) and does not move in with time like in the case without accretion bursts.

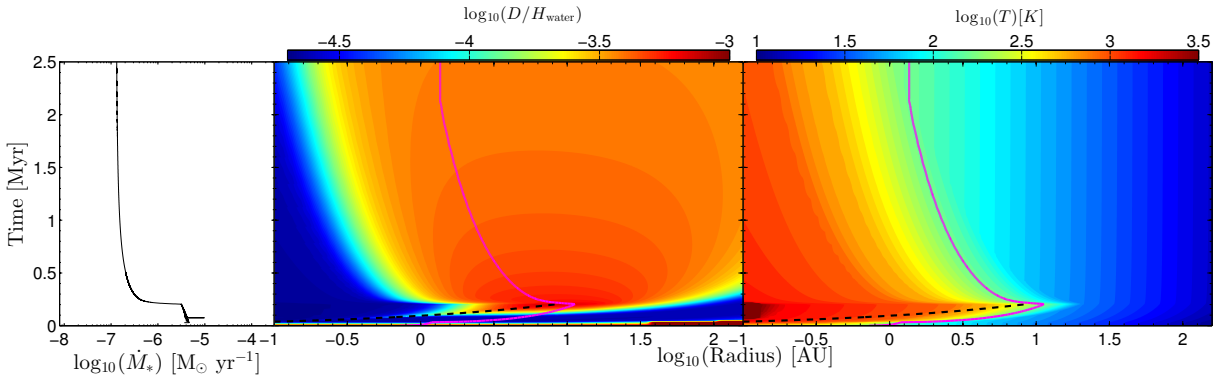


**Figure 7.** Evolution of a disc building calculation calculation with $\Omega_c = 8.88 \times 10^{-15}$ s$^{-1}$, no accretion bursts and a Schmidt number of 1.0. The left-hand panel shows the accretion rate as a function of time. The middle panel is a space-time plot showing the evolution of the $(D/H)_{\rm water}$ ratio and the right panel is a space-time plot for the temperature evolution. The thick solid line shows the time evolution of the water snow-line taken to be at 170 K. The mass evolution of the star, cloud core and disc are shown in the top panel of Figure 6.

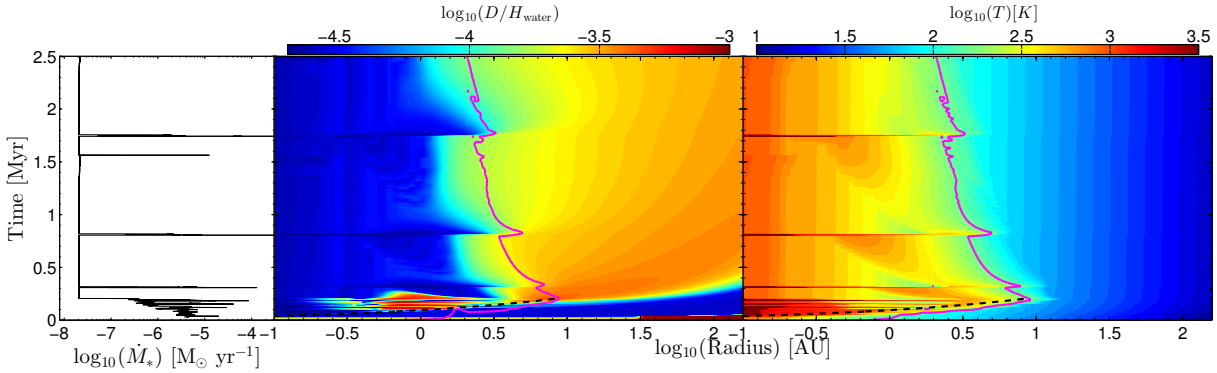


**Figure 8.** Same as Figure 7 for a disc building calculation calculation with $\Omega_c = 8.88 \times 10^{-15}$ s$^{-1}$, accretion bursts and a Schmidt number of 1.0. The mass evolution of the star, cloud core and disc are shown in the bottom panel of Figure 6.

The evolution of the $(\rm D/H)_{water}$ profile during an accretion burst is shown in Figure 9. where the solid line shows the $(\rm D/H)_{water}$ profile just prior to an accretion burst and the dashed line shows the $(\rm D/H)_{water}$ profile just after an accretion outburst. We see that the outburst equilibrates water in the dead zone ($\sim 0.5 - 3$ AU), decreasing the overall $(\rm D/H)_{water}$ ratio of the entire disc. This newly equilibrated disc material is then transported by advection to smaller radius and to large radius by turbulent diffusion. This diffusion of newly equilibrated water to large radius results in a lower $(\rm D/H)_{water}$ ratio at large radii in the disc, explaining lower peak $(\rm D/H)_{water}$ ratios compared to burst-free models.

### 4.2 Parameter study

In Figure 10, we show how the core's rotation rate effects the $(\rm D/H)_{water}$ profile. We plot the $(\rm D/H)_{water}$ ratio for calculations with a Schmidt number of 1, both with (dashed) and without (solid) accretion bursts at 1, 3, 10 & 30 AU after 1 Myr of evolution. These show that there is a critical rotation rate below which the entire disc is equilibrated of $\sim 3 \times 10^{-15}$ s$^{-1}$ for the calculations without accretion bursts, and $\sim 6 \times 10^{-15}$ s$^{-1}$ for the calculations with accretion bursts, corresponding to maximum centrifugal radii of $\sim 1$ AU and $\sim 4$ AU, respectively (see equation (17)). Below these critical rotation rates all infalling material lands in regions of the disc where the temperature is above the equilibration temperature.

In the cases with accretion bursts at all rotation rates we find that at radii of $\sim 1$ AU the water is equilibrated, unlike the case without accretion burst where above the critical core rotation rate it returns to near primordial values. At large radii the trend seen from the steady infall calculations is also repeated here, where accretion bursts results in a lower $(\rm D/H)_{water}$ ratio; however, the effect is less pronounced. We note the variability seen in the 1.0 & 3.0 AU is indicative of the variability in the $(\rm D/H)_{water}$ ratio with time, in the case with accretion bursts.

Finally, in Figure 11 we show the impact of the Schmidt number on the $(\rm D/H)_{water}$ profile, where we plot our the $(\rm D/H)_{water}$ ratio as a function of radius in our calculations with $\Omega_c = 3.16 \times 10^{-12}$ s$^{-1}$ after 1 Myr of evolution with Schmidt numbers of 0.1 (dashed), 1.0 (solid) & 10.0 (dot-dashed). The top panel shows the calculation without accretion bursts and the bottom panel shows the calculations with accretion bursts. At small Schmidt numbers there is enhanced transport of equilibrated water to large radius resulting in a lower $(\rm D/H)_{water}$ ratio at large radius (as

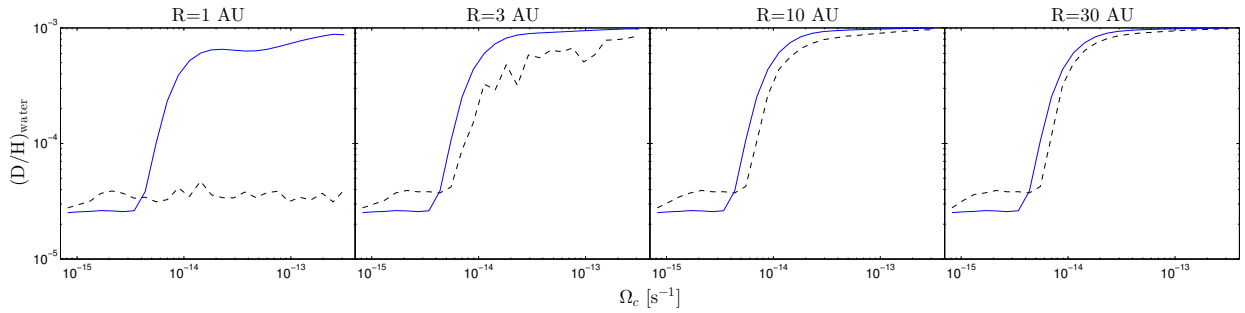


**Figure 10.** The $(D/H)_{water}$ ratio as a function of the cloud core rotation rate ($\Omega_c$). The solid lines show calculations without accretion bursts and the dashed lines show calculations with accretion bursts, shown after 1 Myr of evolution. The four panels from left to right show disc radii of 1.0, 3.0, 10.0 & 30.0 AU. All calculations used a Schmidt number of unity. The variation at small radius in the calculations with accretion bursts is a measure of the time-variability due to the variability due to the bursts.

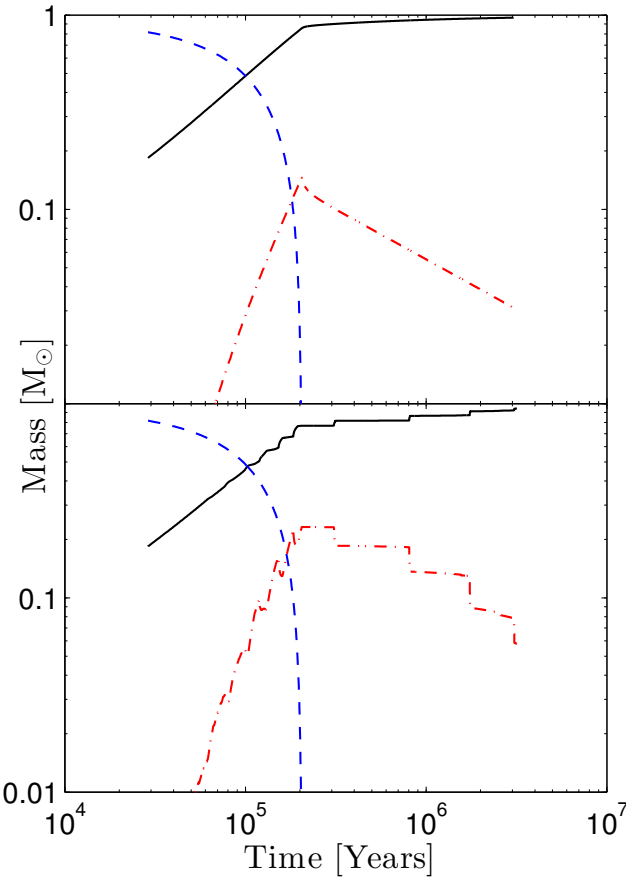


**Figure 6.** The mass in the three components as a function of time: star (solid), cloud core (dashed) and disc (dot-dashed). The top panel shows a calculation with no accretion bursts and the bottom panel shows a calculation with accretion bursts. Both calculations have $\Omega_c = 8.88 \times 10^{-15}$ s$^{-1}$ and a Schmidt number of unity.

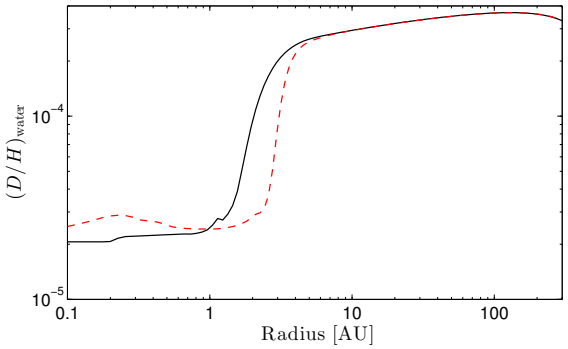


**Figure 9.** The $(D/H)_{water}$ profile just before (0.795 Myr, solid) and after (0.819 Myr, dashed) an accretion burst. Shown for the simulation with $Sc = 1.0$ and $\Omega_c = 8.88 \times 10^{-15}$ s$^{-1}$ where the accretion burst occurs at ∼0.8 Myr (see Figure 8).

seen by Jacquet & Robert 2013). Conversely, larger Schmidt numbers result in sharper transitions from the equilibrated water to the primordial value outward as expected from the reduced efficiency of turbulent diffusion (e.g. Jacquet & Robert 2013; Owen 2014b).

## 5 DISCUSSION

Our calculations have shown that the presence of dead zones in protoplanetary discs, which can give rise to accretion bursts have a significant impact on the evolution of the $(D/H)_{water}$ ratio in water. This is not surprising since the $(D/H)_{water}$ ratio equilibrates at temperatures $> 400-800$ K (Jacquet & Robert 2013; Yang, Ciesla, & Alexander 2013) which lies in-between the quiescent temperature of the dead-zone of $\sim 200$ K and the dead-zone temperature during an accretion burst of $\sim 1000$ K. Hence, un-equilibrated material that resides in the dead zone prior to an accretion burst is brought closer to equilibration by the higher disc temperatures.

### 5.1 Implications for astrophysical systems

Our calculations have shown that the cloud core's rotation rate plays a strong role in setting the $(D/H)_{water}$ ratio at large radius in the disc. Thus, given the several order of magnitude spread in observed core rotation rates, with typical values $\sim 10^{-14}$ s$^{-1}$ (Goodman et al. 1993; Barranco &

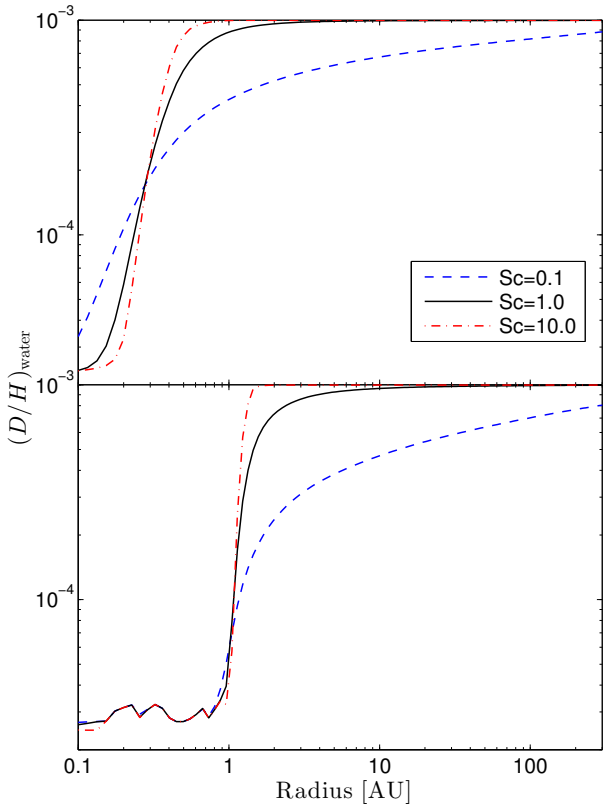


**Figure 11.** $(D/H)_{water}$ ratio as a function of radius for calculations with $\Omega_c = 3.16 \times 10^{-13}$ s$^{-1}$ for Schmidt numbers of 0.1 (dashed), 1.0 (solid) & 10.0 (dot-dashed). The top panel shows calculations without accretion bursts the bottom panel shows calculations with accretion bursts.

Goodman 1998; Caselli et al. 2002) then one would expect to observe a large spread in the $(D/H)_{water}$ values measured at large radii in protoplanetary discs. Therefore, Herschel (e.g. Visser et al. 2013), ALMA or TMT measurements of the $(D/H)_{water}$ ratio would allow inferences about the initial angular momentum of the discs. Additionally, if the $(D/H)_{water}$ ratio could be spatially resolved then the properties of accretion bursts could be probed or spatial variations in the $(D/H)_{water}$ ratio then the probe could be used to place constraints on the Schmidt number, similar to the method detailed by Owen (2014b) for spatial variations at various molecular snow lines. Furthermore, combined observations of the crystalline silicate fraction (e.g. Bouwman et al. 2001) and $(D/H)_{water}$ ratio would allow the outward transport of crystalline materials by decretion during disc building hypothesis (e.g. Dullemond, Apai, & Walch 2006) to be tested. Indeed discs with high crystallinity fractions at large radius should also possess lower $(D/H)_{water}$ ratios.

Thus, future observations of the $(D/H)_{water}$ ratio should be able to probe the angular momentum distribution of the disc during the its building and formation. Additionally, spatially resolved observations of the $(D/H)_{water}$ ratio should be able to determine whether the majority of protoplanetary discs experienced accretion bursts during their early evolution.

### 5.2 Solar system constraints

To first order, the D/H systematics in the solar system may be subsumed in two salient features (Robert et al. 2006; Ceccarelli et al. 2014):

(i) Most Oort cloud comets show $(D/H)_{water}$ values of $\sim 3 \times 10^{-4}$ (with some comets showing lower values), lower than expected in molecular clouds.
(ii) Carbonaceous chondrites display D/H ratios significantly lower than cometary (around the terrestrial value $1.5 \times 10^{-4}$).

Both domains of variation are significantly higher than the protosolar value ($2 \times 10^{-5}$) and significantly lower than the value observed in molecular clouds ($\gtrsim 10^{-3}$).

In our framework, fact (i) indicates that infall has occurred on relatively small radii to allow significant equilibration before outward transport, which, as mentioned in the previous subsection, would also account for the presence in comets of crystalline silicates, also deemed to have originated in the inner solar system (Dullemond, Apai, & Walch 2006). At the same time, the relatively large D/H ratio of cometary water compared to the protosolar value suggests that equilibration has not been complete. Judging from Figure 10, that would at face value constrain the rotation rate to be within a factor of several of $10^{-14}$ s$^{-1}$ (with a factor of $\sim 2$ systematic difference between the outburst-free and outburst-laden cases). Of course, the infall model is very idealized, so the situation may not be as fine-tuned as it may seem (whether with or without outbursts, incidentally). It is also possible that comets, whose $(D/H)_{water}$ is somewhat variable, do not mark the *peak* $(D/H)_{water}$ value of the disc, and whatever that may be, this latter value may still be consistent with the lower end of those determined for prestellar cores (e.g. Ceccarelli et al. 2014).

The importance of fact (ii) may be grasped from examination of Figure 12 which plots $(D/H)_{water}$ against the disc temperature for various disc models, along with the aforementioned solar system data. The dashed line shows the curve for a simulation without outbursts $\Omega_c = 7 \times 10^{-15}$ s$^{-1}$ and a Schmidt number of 1, for which the maximum D/H ratio roughly matches that displayed by comets at large radii ($\gtrsim 10$ AU). It is seen that at the snow line (taken here to correspond to a temperature of 170 K), $(D/H)_{water}$ is not very different from this maximum value, that is, in this case diffusion of equilibrated water from the inner solar system is too inefficient to induce a substantial deviation. However, carbonaceous chondrites, which generally show ample evidence of aqueous alteration and therefore initial presence of ice, should have formed beyond the snow line, and yet their D/H ratio is much lower than this. This Jacquet & Robert (2013) pointed out as a general problem of standard disc models with $Sc \gtrsim 1$. However, Jacquet & Robert (2013) noted that assuming a Schmidt number of about 0.2 (more efficient turbulent diffusion), would alleviate this discrepancy, as illustrated by their analytic profile (in a quasi-static approximation) plotted as a red dot-dashed line in the figure[2]. While non-MRI and non-ideal turbulence may produce

[2] Note: Jacquet & Robert (2013) adopt a different opacity and viscosity structure to our calculations. We have thus recalculated the equilibration temperature given by Jacquet & Robert using

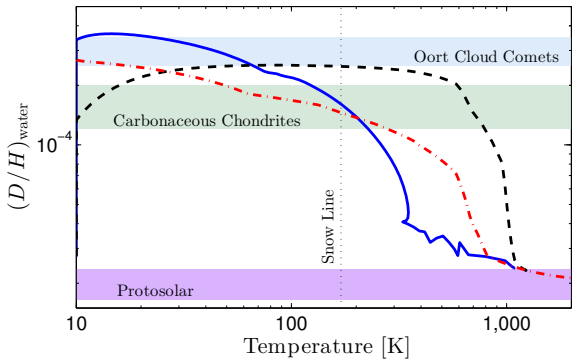


**Figure 12.** The $(D/H)_{water}$ ratio shown against temperature after 1 Myr of evolution. Compared to several solar-system constrains: protosolar (e.g. Geiss & Gloeckler 2003), carbonaceous chondrites (e.g. Alexander, Bonal, & Sutton 2012) and the majority of Oort cloud comets (e.g Bockelée-Morvan et al. 2009, 2012). The snow-line at a temperature of 170 K is marked with the thin vertical dotted line. The thick solid line shows a simulation with $Sc = 1.0$, accretion bursts and $\Omega_c = 8.88 \times 10^{-15}$ s$^{-1}$. The thick dashed line shows a simulation with $Sc = 1.0$, no accretion bursts and $\Omega_c = 7 \times 10^{-15}$ s$^{-1}$. The thick dot-dashed line corresponds to the best fit solution of Jacquet & Robert (2013) with $Sc = 0.16$.

Sc values $\lesssim 1$ (e.g. Prinn 1990; Zhu, Stone, & Bai 2014), it is unclear how realistic such low Schmidt numbers are, and the required Sc values could be yet lower if the D/H values displayed by carbonaceous chondrite clays were compromised by isotopic exchange with organic matter as suggested by Alexander, Bonal, & Sutton (2012). If we now allow for bursts, the situation changes: the solid blue line in Figure 12 stands for a simulation with bursts ($\Omega_c = 8.88 \times 10^{-15}$ s$^{-1}$) also matching the cometary $(D/H)_{water}$ value at large radii, but this time matching the chondritic value at the snow line, despite a Schmidt number of 1. This is because accretion bursts have been able to process water in the inner disc, affecting the snow line, but the $(D/H)_{water}$ value at large radii has not evolved in pace with it (see also Figure 9). So this may be an alternative way to account for the low D/H ratios of carbonaceous chondrites.

To summarize, in order to explain the distribution of $(D/H)_{water}$ ratios measured in carbonaceous chondrites and comets we need that either: (i) the turbulent transport occurs with a rather low Schmidt number $\sim$ 0.2, and the disc did not experience accretion bursts (Jacquet & Robert 2013); or (ii) turbulent transport occurs with a nominal Schmidt number of $\sim$ 1 and the disc experiences several accretion bursts during the initial stages of its evolution.

### 5.3 Caveats and avenues for further work

While we have shown that accretion bursts can have a significant impact on the evolution of the $(D/H)_{water}$ ratio, our results cannot be considered precise predictions. Rather, our simple models have allowed us to explore a large parameter space. Thus, we must discuss the impact our simplifications may have had on the evolution. In particular, we adopted a rather simple model for the chemical evolution of the water and integrated one rate equation instead of a large chemical network; however, we have shown our method agrees well with the more detailed calculations of Yang, Ciesla, & Alexander (2013), although reactions not considered by the latter (e.g. ion-neutral) could be important (Albertsson, Semenov, & Henning 2014).

Perhaps the biggest simplification is the use of a one-dimensional, one-layer model, where the evolution is controlled by the properties at the mid-plane of the disc. Yang, Ciesla, & Alexander (2013) performed a series of simulations where they considered the impact of the vertical temperature structure on the evolution of the $(D/H)_{water}$ ratio and found it to be negligible. However, this may not be true for the layered structure in the dead-zone where the active surface layers that contain little mass, have a temperature different from the more massive dead zone (Bae et al. 2013a; Martin & Lubow 2014) and there may be turbulent mixing between the active and dead layers, with the possibility that the dead zone itself contains residual levels of turbulence (e.g. Fleming & Stone 2003; Turner, Carballido, & Sano 2010; Okuzumi & Hirose 2011). Such a 2D structure would be worth taking into account.

We have also assumed throughout the paper that water was tightly coupled to the gas. However, this may not be true at large distances (where water is solid) and late stages of the disc's evolution, especially if water becomes incorporated in growing aggregates of mm to m size (e.g. Ciesla & Cuzzi 2006). It might be *a priori* expected that the effect will be to make outward transport of equilibrated water more difficult (Jacquet & Robert 2013) but simulations including gas-solid drift, accretion and fragmentation would be worthwhile to address the effect on the $(D/H)_{water}$ ratio.

Finally, since we have shown (in agreement with Yang, Ciesla, & Alexander 2013) that the radius and time at which infalling material reaches the disc plays an important role in the late time $(D/H)_{water}$ profile, then more realistic disc formation models should be considered that account for differential rotation and turbulence in the cloud core, as well as the two- (and possibly three-) dimensional nature of the infall onto the disc (Visser et al. 2009; Visser, Doty, & van Dishoeck 2011), along with the associated angular momentum mis-match that can occur between the Keplerian disc rotation and the rotation rate of the infalling material.

## 6 CONCLUSIONS

We have used a 1D model of a layered protoplanetary disc that undergoes accretion bursts due to the gravo-magnetic limit cycle (a commonly invoked mechanism to explain FU Orionis outbursts) to study their impact on the $(D/H)_{water}$ ratio. We have performed two types of calculations; firstly, a set of calculations with a steady infall rate onto the disc where we vary the infall rate, infall radius, Schmidt number, Prandtl number and whether or not the disc contains a dead zone. Secondly, we perform a series of calculation where we build the disc and star from a uniformly rotating isothermal cloud core, where we vary the rotation rate,

our opacity and viscosity choices and obtain 777 K instead of 500 K. The best fit Schmidt number is however only slightly changed from 0.20 to 0.16 as the reduction of the equilibration radius is somewhat compensated by the lower equilibrium $(D/H)_{water}$ (at higher temperatures) there.

Schmidt number and whether the disc contains a dead zone. In all these calculations we find that accretion burst play a major role in equilibrating water with the surrounding hydrogen gas. Thus, the $(D/H)_{water}$ ratio carries an imprint of whether the disc experienced accretion bursts or not. Our main findings are as follows:

(i) During an accretion burst, water in the dead zone region is equilibrated, lowering its D/H ratio to $\sim 2 \times 10^{-5}$, as the dead zone temperature reaches $\sim 1000$ K during the accretion burst, higher than the equilibration temperature.

(ii) Discs that undergo accretion bursts have, in general, lower $(D/H)_{water}$ ratios as the burst thermally process a larger fraction of the disc material. Equilibrated water from the accretion burst can be carried to large radius by diffusion resulting in lower D/H ratios at 10-100s of AU.

(iii) Discs that undergo accretion bursts have larger equilibration radii (1-5 AU) compared to discs that do not experience accretion bursts.

(iv) The rotation rate of the parent cloud core plays an important role in setting the large scale $(D/H)_{water}$ profile as suggested by Yang, Ciesla, & Alexander (2013), indicating there should be a significant variation in the D/H ratio in protoplanetary discs.

(v) Agreement with the solar-system constraints requires, either: (1) the solar nebula experienced no accretion bursts and had a low Schmidt number $\lesssim 0.2$; or (2) the solar nebula experienced accretion bursts and had a Schmidt number close to "nominal" (i.e. unity).

Given the important role of accretion bursts in the evolution of $(D/H)_{water}$, we suggest more detailed modelling of their impact on the chemical and physical evolution of protoplanetary discs be performed. Finally, coupling these models with future observations, the $(D/H)_{water}$ ratio and profile could be used as probe for the prevalence of accretion bursts in the earliest stages of protoplanetary disc evolution.

## ACKNOWLEDGEMENTS

We thank the referee for comments which improved the paper. We are grateful to Phil Armitage for useful discussions. The numerical calculations were performed on the Sunnyvale cluster at CITA, which is funded by the Canada Foundation for Innovation.

## APPENDIX A: NUMERICAL TEST

Since we have adopted a simplified approach to the chemical evolution in view of the numerous chemical reactions that may govern evolution of the deuterium fraction in water, we need to test whether our method is appropriate for studying the effect of accretion bursts. Therefore, we repeat the 'standard model' of disc evolution calculation of Yang, Ciesla, & Alexander (2013) who include a much more complete chemical network with 14 species and 48 reactions. The model parameters are described in Table 3 of Yang, Ciesla, & Alexander (2013) (i.e. $\Omega_c = 10^{-14}$ s$^{-1}$, $T_c = 15$ K & $\alpha = 0.001$). However, we do not simplify our temperature solver and opacity structure to that used by Yang & Ciesla (2012); Yang, Ciesla, & Alexander (2013), but rather use the more detailed method described in Section 2. The results of our calculation are shown every 0.05Myr in the left hand panel of Figure A1 and the results from the Yang et al.'s original calculation are shown in the right-hand panel at 0.1, 0.2, 0.3, 0.5 & 1.0 Myr.

We see that the two evolutionary paths agree very well, particularly at late times (which we are primarily interested in from the point of view of observables). This indicates that our simple method for calculating the evolution $(D/H)_{water}$ ratio produces results comparable with the more detailed chemical method used by Yang, Ciesla, & Alexander (2013). This is not surprising since Yang, Ciesla, & Alexander (2013) performed a detailed exploration of the different approaches for the chemical evolution and found they gave similar results. Therefore, we are confident that our method is suitable for exploring the effect of accretion bursts on the D/H ratio in water.

## REFERENCES

Albertsson T., Semenov D., Henning T., 2014, ApJ, 784, 39
Alexander C. M. O., Bonal L., Sutton S., 2012, M&PSA, 75, 5297
Armitage P. J., Livio M., Pringle J. E., 2001, MNRAS, 324, 705
Audard, M., et al., 2014, to appear in Protostars and Planets VI, eds. H. Beuther, R. Klessen, C. Dullemond, Th. Henning, University of Arizona Press (arXiv:1401.3368)
Bouwman J., Meeus G., de Koter A., Hony S., Dominik C., Waters L. B. F. M., 2001, A&A, 375, 950
Bae J., Hartmann L., Zhu Z., Gammie C., 2013, ApJ, 764, 141
Bae, J., Hartmann, L., Zhu, Z., Gammie, C., 2013, ApJ, 764, article id. 141
Balbus, S. A., Hawley, J. F., 1998, Reviews of Modern Physics, 70, 1
Barranco J. A., Goodman A. A., 1998, ApJ, 504, 207
Bockelée-Morvan D., Woodward C. E., Kelley M. S., Wooden D. H., 2009, ApJ, 696, 1075
Bockelée-Morvan D., et al., 2012, A&A, 544, L15
Bell K. R., Cassen P. M., Klahr H. H., Henning T., 1997, ApJ, 486, 372
Caselli P., Benson P. J., Myers P. C., Tafalla M., 2002, ApJ, 572, 238
Ceccarelli C., Caselli P., Bockelee-Morvan D., Mousis O., Pizzarello S., Robert F., Semenov D., 2014, to appear in Protostars and Planets VI, eds. H. Beuther, R. Klessen, C. Dullemond, Th. Henning, University of Arizona Press (arXiv:1403.7143)
Chiang E. I., Goldreich P., 1997, ApJ, 490, 368
Ciesla F. J., Cuzzi J. N., 2006, Icar, 181, 178
D'Alessio P., Calvet N., Hartmann L., 2001, ApJ, 553, 32
Deloule E., Robert F., Doukhan J. C., 1998, GeCoA, 62, 3367
Drouart A., Dubrulle B., Gautier D., Robert F., 1999, Icar, 140, 129
Dullemond C. P., Natta A., Testi L., 2006, ApJ, 645, L69
Dullemond C. P., Apai D., Walch S., 2006, ApJ, 640, L67
Durisen R. H., Boss A. P., Mayer L., Nelson A. F., Quinn T., Rice W. K. M., 2007, Protostars & Planets V, 607

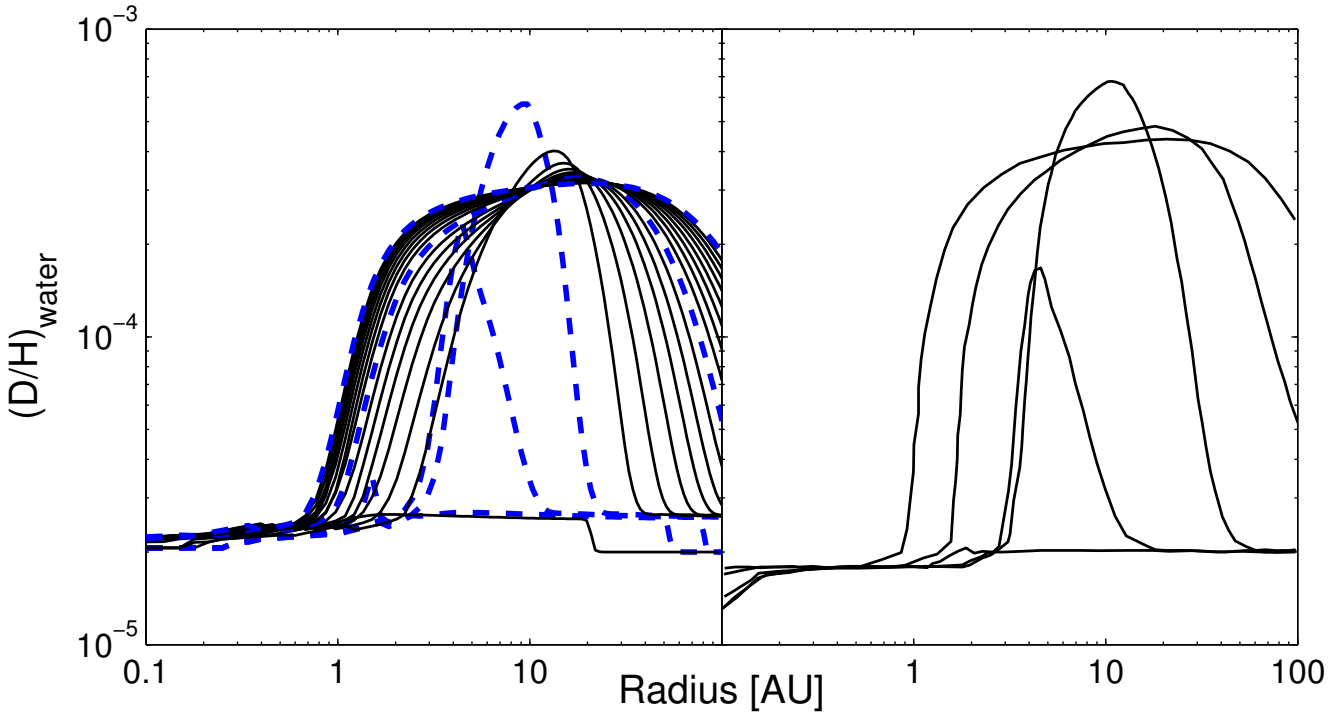


**Figure A1.** Results of the benchmarking calculation. The left-hand panel shows the $(D/H)_{water}$ ratio plotted every 0.05 Myr from our calculation. The right-hand panel shows the results from the Yang, Ciesla, & Alexander (2013) calculation (their 'standard model' shown in Figure 4 of Yang, Ciesla, & Alexander 2013) with the $(D/H)_{water}$ ratio plotted at 0.1, 0.2, 0.3, 0.5 & 1.0 Myr. To ease comparison, we indicate the same times shown for the Yang et al. calculation in our calculation by plotting those times as thick dashed lines, rather than solid lines.


Ercolano B., Mayr D., Owen J. E., Rosotti G., Manara C. F., 2014, MNRAS, 439, 256
Evans N. J., II, et al., 2009, ApJS, 181, 321
Fleming T., Stone J. M., 2003, ApJ, 585, 908
Gammie C. F., 1996, ApJ, 457, 355
Geiss J., Gloeckler G., 2003, SSRv, 106, 3
Goodman A. A., Benson P. J., Fuller G. A., Myers P. C., 1993, ApJ, 406, 528
Hartmann L., Calvet N., Gullbring E., D'Alessio P., 1998, ApJ, 495, 385
Hartmann, L., Kenyon, S. J., 1996, ARA&A, 34, 207
Hässig M., et al., 2013, P&SS, 84, 148
Hersant F., Gautier D., Huré J.-M., 2001, ApJ, 554, 391
Hogerheijde M. R., et al., 2011, Sci, 334, 338
Hueso R., Guillot T., 2005, A&A, 442, 703
Jacquet E., Robert F., 2013, Icar, 223, 722
Kenyon S. J., Hartmann L., 1987, ApJ, 323, 714
Kenyon, S. J., Hartmann, L. W., Strom, K. M., Strom, S. E., 1990, AJ, 99, 869
Kenyon S. J., Hartmann L., 1995, ApJS, 101, 117
Kim H. J., et al., 2011, ApJ, 729, 84
Kim H. J., Evans N. J., II, Dunham M. M., Lee J.-E., Pontoppidan K. M., 2012, ApJ, 758, 38
Lasota, J.-P., 2001, New Astronomy Reviews, 45, 449
Lécluse C., Robert F., 1994, GeCoA, 58, 2927
Lee J.-E., 2007, JKAS, 40, 83
Lin D. N. C., Pringle J. E., 1987, MNRAS, 225, 607
Lin D. N. C., Pringle J. E., 1990, ApJ, 358, 515
Lodato G., Rice W. K. M., 2004, MNRAS, 351, 630
Lodato G., Rice W. K. M., 2005, MNRAS, 358, 1489
Martin R. G., Lubow S. H., 2011, ApJL, 740, article id. L6
Martin R. G., Lubow S. H., 2013, MNRAS, 432, 1616
Martin R. G., Lubow S. H., 2014, MNRAS, 437, 682
Mohanty S., Ercolano B., Turner N. J., 2013, ApJ, 764, 65
Mousis O., Gautier D., Bockelée-Morvan D., Robert F., Dubrulle B., Drouart A., 2000, Icar, 148, 513
Ohtani T., Kimura S. S., Tsuribe T., Vorobyov E. I., 2014, arXiv, arXiv:1408.5596
Okuzumi S., Hirose S., 2011, ApJ, 742, 65
Owen J. E., 2014a, ApJ, 789, 59
Owen J. E., 2014b, ApJ, 790, L7
Owen J. E., Armitage P. J., 2014, MNRAS, 445, 2800
Piani L., 2012, Origine des éléments volatils dans le système solaire: la matiére organique et les argiles des chondrites, PhD Thesis, Museum National d'Histoire Naturelle
Piani L., Robert F., Rémusat L., 2014, Earth and Planetary Science Letters *submm.*
Prinn R. G., 1990, ApJ, 348, 725
Richet P., Bottinga Y., Janoy M., 1977, AREPS, 5, 65
Robert F., Mostefaoui S., Aléon J., Derenne S., Remusat L., Meibom A., 2006, LPI, 37, 1301
Shakura N. I., Sunyaev R. A., 1973, A&A, 24, 337
Shu F. H., 1977, ApJ, 214, 488
Toomre A., 1964, ApJ, 139, 1217
Turner N. J., Carballido A., Sano T., 2010, ApJ, 708, 188
van Dishoeck, E., Bergin, T., Lis, D., Lunine, J. 2014, to appear in Protostars and Planets VI, eds. H. Beuther, R. Klessen, C. Dullemond, Th. Henning, University of Ari-

zona Press (arXiv:1401.8103)
Visser R., van Dishoeck E. F., Doty S. D., Dullemond C. P., 2009, A&A, 495, 881
Visser R., Doty S. D., van Dishoeck E. F., 2011, A&A, 534, A132
Visser R., Bergin E. A., 2012, ApJ, 754, L18
Visser R., Jørgensen J. K., Kristensen L. E., van Dishoeck E. F., Bergin E. A., 2013, ApJ, 769, 19
Vorobyov E. I., Baraffe I., Harries T., Chabrier G., 2013, A&A, 557, A35
Yang L., Ciesla F. J., 2012, M&PS, 47, 99
Yang L., Ciesla F. J., Alexander C. M. O. '., 2013, Icar, 226, 256
Zhu Z., Hartmann L., Gammie C. F., Book L. G., Simon J. B., Engelhard E., 2010, ApJ, 713, 1134
Zhu Z., Hartmann L., Gammie C., 2010, ApJ, 713, 1143
Zhu, Z., Hartmann, L., Gammie, C., McKinney, J. C., 2009, ApJ, 701, 620
Zhu Z., Stone J. M., Bai X.-N., 2014, arXiv, arXiv:1405.2778